NEAR-REAL TIME FLOOD EXTENT MONITORING IN MARIKINA RIVER PHILIPPINES: MODEL PARAMETERISATION USING REMOTELY-SENSED DATA AND FIELD MEASUREMENTS

Jojene R. Santillan, Enrico C. Paringit, Roseanne V. Ramos
Research Laboratory for Applied Geodesy and Space Technology, Training Center for Applied Geodesy and Photogrammetry & Department of Geodetic Engineering, University of the Philippines, Diliman, Quezon City, Philippines; Tel: +63-2-9818500 ext. 3147; E-mail: jrsantillan@up.edu.ph; paringit@gmail.com

John Robert T. Mendoza, Nena Carina Española
Grid Operations Team, Advance Science and Technology Institute, Department of Science and Technology, C.P. Garcia Avenue, Technology Park Complex, UP Campus, Diliman, Quezon City, Philippines; Tel: +63-2-4269760

Jen Alconis
National Institute of Geological Sciences, University of the Philippines, Diliman, Quezon City, Philippines

KEY WORDS: Flood extent monitoring, HEC RAS, ALOS AVNIR2, Marikina River, Philippines.

ABSTRACT: Floods are a persistent problem in the Philippines that need to be addressed in a more scientific way in order to mitigate its costly impacts to human lives and properties. The September 2009 floods caused by Typhoon Ketsana that devastated Metro Manila and its surroundings exemplified the need for an accurate and reliable flood monitoring tool for determining the extents of floods and for assessing the risks due to this disaster. In this study, we developed and parameterized a near-real time flood extent monitoring model for Marikina River, Philippines using the Hydrologic Engineering Center – River Analysis System (HEC RAS) program. River bathymetric surveys and cross-section measurements were conducted to generate the geometry of the Marikina River required by HEC RAS. Flood plain surface roughness coefficients needed to parameterize the model were derived from multispectral classification of a 10-m spatial resolution ALOS AVNIR-2 of the study area. The HEC RAS model was configured to accept real time 10-minute water level data from the Enhanced Flood Control and Operation Warning System (EFCOS) monitoring stations along the Marikina River as model boundary conditions. Automation scripts were used to convert the time series of water level data from the stations to a format that could be readily used by the HEC RAS model. An automation script was also developed for running the HEC RAS modeling workflow without human intervention such as assigning of model initial and boundary conditions, setting of simulation time window, model computation and generation of flood extent and flood depths. The outputs generated are then uploaded automatically to the Project NOAH (Nationwide Operational Assessment of Hazards) website where the public could view in near real-time the flooding extent along Marikina River. This near-real time generation of flood maps could be useful in providing information to the public as to the possible extent and depth of flooding in the Marikina River that could then assist in preparation for evacuation. Validation of the model using time series of water level data for two rainfall events showed an average error of -16 cm and root mean square error of 25 cm. The model has a Nash-Sutcliffe Coefficient of Model Efficiency (E) of 0.88 which signifies satisfactory model performance but requires further improvement and calibration. The study proves the usefulness of remote sensing and GIS technologies in model preparation and parameterizations, as well as in providing near-real time outputs for viewing by the public.

1. INTRODUCTION

Floods are a persistent problem that needs to be addressed in a more scientific way in order to mitigate its costly impacts to properties and human lives. In the Philippines, the September 2009 flooding caused by Tropical Storm (TS) Ketsana (Local Name: *Ondoy*) that devastated Metro Manila and its surroundings (Abon et al., 2011) exemplified the need for an accurate and reliable flood monitoring tool for determining the possible duration and extents of floods and for assessing the risks due to this disaster. It can be recalled that on September 26, 2009, TS Ketsana dumped a month's worth of rain in less than 24 hours and caused flooding in Metro Manila, killing at least 300 people and displacing another 700,000 (Cheng, 2009).

One of the rivers that overflowed and resulted to exceptionally high and extensive flooding during the TS Ketsana event is Marikina River (Figure 1). This river, with an approximate length of 31 km, drains the 582 km^2 Marikina River Basin (MRB) towards the Pasig River (Abon et al., 2011). The river traverses a highly urbanized floodplain wherein the portions of the Rizal Province, Quezon City, Marikina City and Pasig City are situated. As the flood

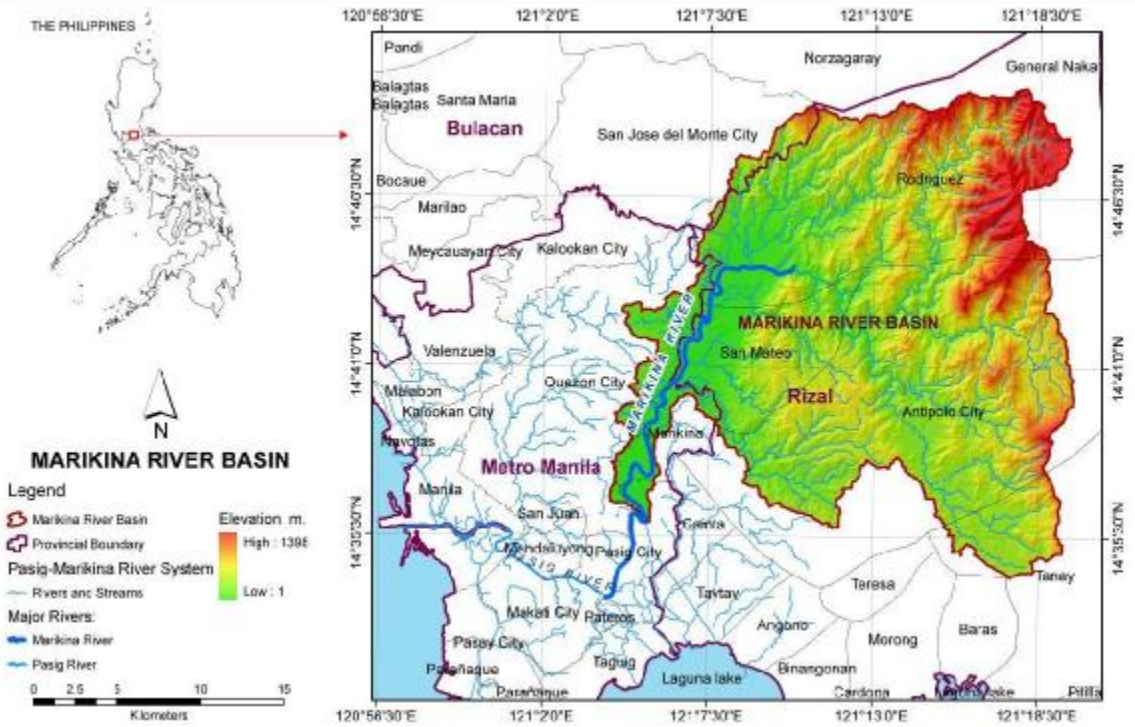

Figure 1. Map showing the location of the Marikina River Basin.

plain is host to densely populated areas as well as commercial and industrial zones, flooding due to overflowing of the river will result to significant damage to human lives and properties.

Some studies have been conducted to understand flooding in the Marikina River (Badilla, 2008; Abon et al., 2011). Several water level and rainfall monitoring stations are also in place in the MRB and along the Marikina River that can provide an up-to-date status of water levels at selected sections of the main river, and of rainfall depth at different locations within MRB. However, these efforts appear to be lacking in terms of providing near-real time information on the status of water levels all throughout the river, especially if one wanted to know the current extent of flooding along the river and the areas that are presently flooded. Providing this kind of information during a heavy rainfall event is useful in informing the public as to the current extent and depth of flooding in the Marikina River that could then assist in preparation for evacuation. This will also aid in estimating the severity of damage as flooding progresses.

In this paper, we present the development of a near-real time flood extent monitoring system for Marikina River. We emphasize the use remote sensing and GIS technologies, together with field measurements, in model preparation and parameterizations, as well as in providing near-real time outputs for viewing by the public.

Figure 2. A close-up view of the Marikina River. Shown is the flood model domain extent.

2. STUDY AREA

The flood extent monitoring system was developed for the section of the Marikina River starting from San Jose Bridge, Montalban, Rizal province in the upstream, and at Rosario junction in Pasig City at the downstream (Figure 2). The length covered is approximately 21.12 km. At these two locations are water level (WL) monitoring stations of the Enhanced Flood Control and Operation Warning System (EFCOS) namely Station MONTALBAN and Station ROSARIO. At about 6.7 km from the

downstream is another EFCOS WL Station named STO. NIÑO. The WL stations are integral to the development of the flood extent monitoring system as they will be the main source of WL information for the flood model simulation. A buffer of 1 km from the river centerline at both banks of the river was set as the flood model domain.

3. METHODS

Figure 3 summarizes the development of the Marikina River Flood Extent Monitoring System. The development consisted of three major steps: flood model setup, flood model automation, and online visualization.

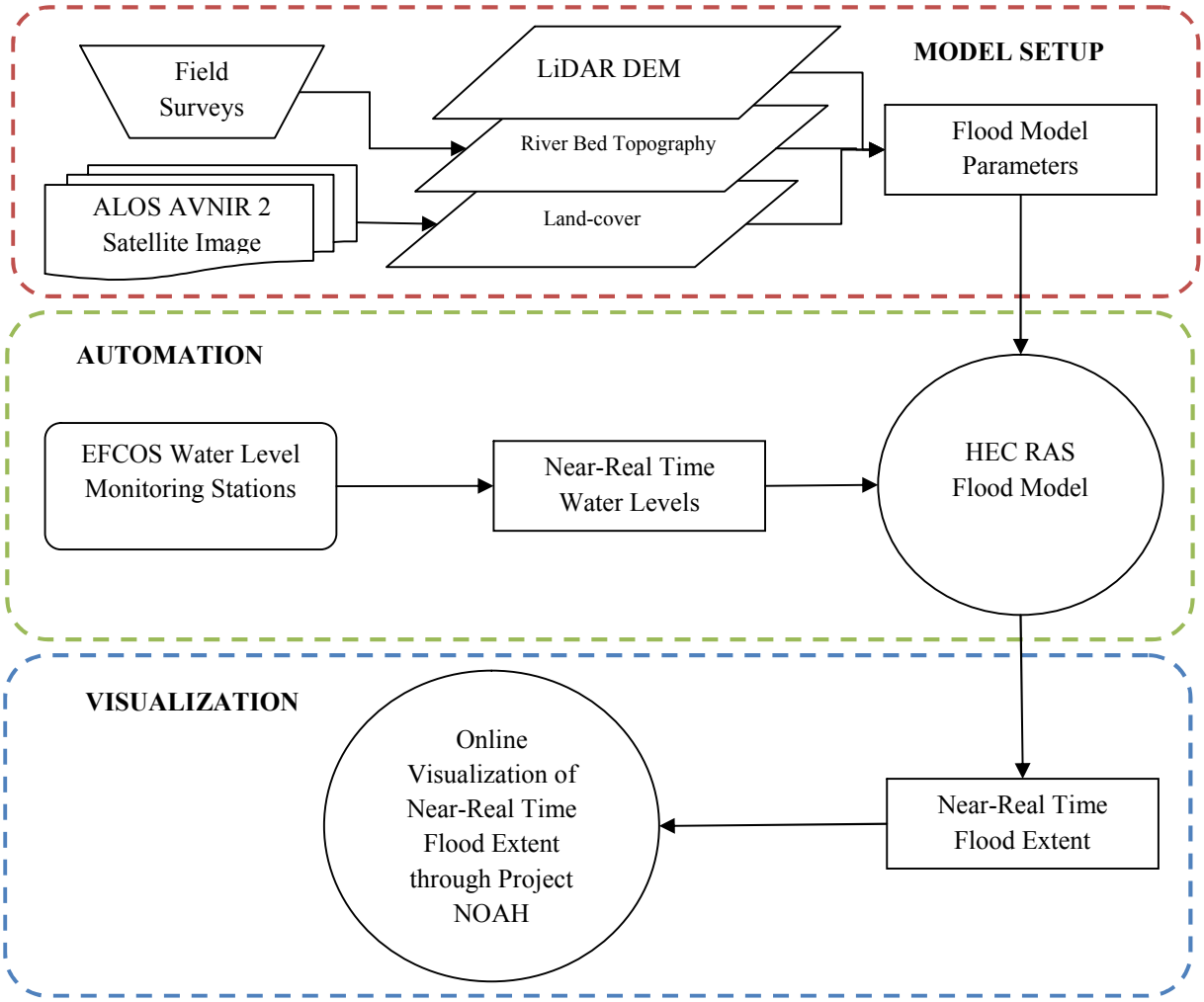

Figure 3. Flow chart showing the development of the Marikina River Flood Extent Monitoring System.

3.1 Model Setup

The Hydrologic Engineering Center – River Analysis System (HEC RAS; Brunner, 2010a) was used in developing the Marikina River Flood Model.

3.1.1 Model Geometry

HEC RAS requires a geometric representation of the river systems in terms of cross-sections, centerline and river banks. The model geometry was prepared using Arcview GIS. River centerlines and banks were digitized from a 1-m resolution digital elevation model derived using Light Detection and Ranging (LiDAR) technology. By creating a hill shade of the DEM, it became easier to digitize the needed geometric information because the banks of the Marikina River are very well defined in the hill shade. However, the river bed in the DEM is poorly represented. It is necessary to supplement the DEM with river bed topography to extract accurate cross-sections. In this study, bed topography of the Marikina River was derived using a Hi-Target single beam echosounder coupled with a dual-

frequency Topcon Hiper GA Global Positioning System (GPS). The echosounder surveys were implemented using real-time kinematic in a zig-zag direction. The GPS and the echosounder independently measure the water surface elevation (WSE) and depth, respectively. At a measurement point, the bed surface elevation is computed as WSE – depth. The WSE measurements are referenced to the Mean Sea Level by first conducting GPS localization through the use of seven control points established around the Marikina River. The bed surface elevation points derived from the echosounder and GPS surveys are then interpolated using kriging technique to produce a continuous surface of the river bed topography at 1-m resolution. This surface was then integrated to the LiDAR DEM. To complete the geometric data requirements of HEC RAS, a total 241 cross-sections were extracted from the updated DEM. Each cross-section is approximately 2 km in length. All the geometric data processing was done using the HEC GeoRAS extension in Arcview GIS 3.2.

3.1.2 Land-cover parameterization based on ALOS AVNIR2 satellite image analysis

As river flow computation in HEC RAS is based on Manning's equation, it is required that surface roughness coefficients be assigned to the channel cross-sections (Brunner, 2010b). For this model parameter, a rectified ALOS AVNIR 2 satellite image acquired on February 2, 2010 with 10-m spatial resolution (Figure 4) was analyzed to derive a land-cover map. This land-cover map was later converted to a surface roughness map by using a look-up table of Manning's roughness coefficients for each class in the land-cover map.

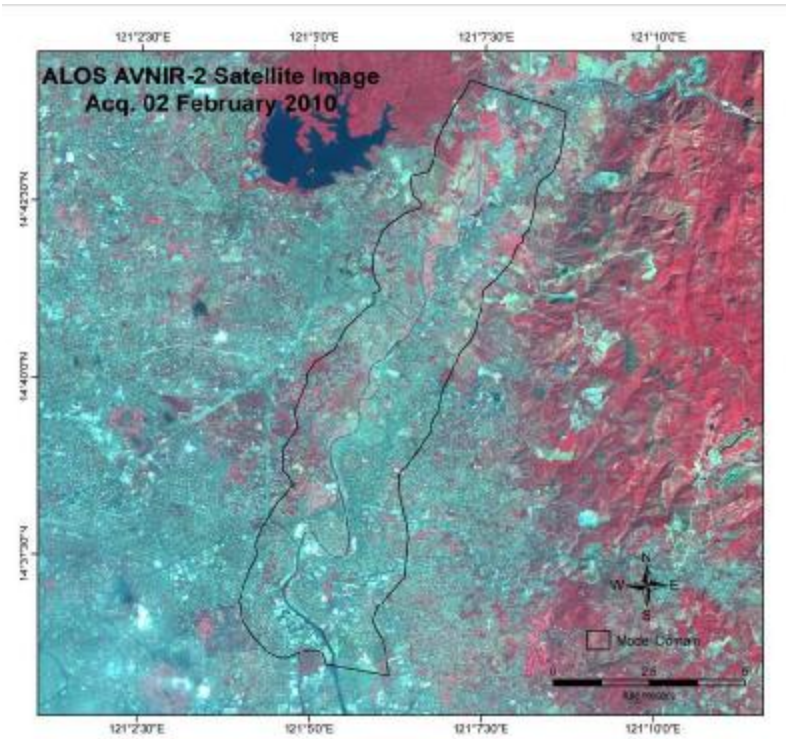

Figure 4. The ALOS AVNIR-2 satellite image (displayed in false color, 4/3/2) acquired on 02 February 2010 that was used to derive land-cover parameters of the HEC RAS model. The flood model domain is enclosed by a polygon with black outline.

The image underwent radiometric calibration by converting the digital numbers (DN) in each band to top-of-atmosphere (TOA) spectral radiance (L_λ), where $L_\lambda = DN_\lambda * Gain_\lambda + Offset_\lambda$. The gain and offset values for each band were obtained from Bouvet et al. (2007). The TOA radiance values were then converted to TOA reflectance for each band (R_λ) using the equation $R_\lambda = \frac{\pi L_\lambda}{E_\lambda \cos\theta}$ where E_λ is the TOA solar irradiance for each band, and θ is the solar zenith angle (39^0) during the time of image acquisition (Bouvet et al., 2007). An atmospheric correction using dark-object subtraction was then applied to the TOA reflectance image. Band ratios (2/3, 2/4) and NDVI bands were then derived from the calibrated and atmospherically-corrected image. These additional bands and a resampled ASTER DEM were layerstacked to the original four bands. The resulting image dataset (referred hereafter as processed ALOS AVNIR-2 image) was used in the land-cover classification using the Maximum Likelihood classifier. The band ratios, NDVI and ASTER DEM were added to increase the number of bands during image classification. The ASTER DEM was added as it has been found that addition of DEMs increases classification accuracy especially in areas of rugged terrain (Elumnoh & Shrestha, 2000). Prior to land-cover classification, clouds and cloud-shadows were removed from the processed image by manual digitizing.

Using high resolution images dated 05 February 2010 that are available in Google Earth, 8 land-cover classes were identified in the processed ALOS AVNIR-2 image. The classes include aquatic vegetation, bare soil, built-up areas, exposed river beds, excavations, dense vegetation (forest), grasslands, and water bodies. Aquatic vegetation, water bodies, exposed river beds and excavations were manually digitized in the processed ALOS AVNIR-2 image to limit the classification to 4 classes. Low classification accuracies were obtained during preliminary supervised classifications when these classes were included. High misclassifications were found for exposed river beds and excavations classes because of the similarity of the spectral reflectance of these classes to built-up areas. For the aquatic vegetation, this class is misclassified as grasslands. The water bodies were manually digitized because it

was desired that rivers and streams be accurately depicted in the resulting land-cover map. For the Maximum Likelihood classification, a training set, with a minimum of 1000 pixels were selected. Another set of randomly selected pixels for each class (but different from the training set) were selected for accuracy assessment. A total of 250 pixels were selected for each class based on the formula of Fitzpatrick-Lins (1981) in determining the minimum number of pixels for classification accuracy assessment given that the desired accuracy is at least 85% at 95% confidence level, and with an allowable margin of error of 5%.

After the Maximum Likelihood classification, all the pixels classified as "dense vegetation" were further subdivided into high density shrubs and trees, medium density shrubs and trees, and low density shrubs and trees. This further classification of the dense vegetation class was necessary to have a detailed land-cover map and surface roughness map. Using only the dense vegetation class will lead to difficulty in assigning the Manning's roughness coefficient because of unavailability of look-up table of roughness value for this particular class. The dense vegetation reclassification was done using K-means with the NDVI band as input. The K-means classifier groups the NDVI values into 3 classes that will correspond to low, medium and high NDVI values. It is assumed that high density shrubs and trees will have high NDVI values while the low density shrubs and trees will have low NDVI values. After this, the land-cover map is finalized by integrating the re-classified dense vegetation class, and the land-cover classes that were digitized earlier. This was then converted to a surface roughness map using a look-up table (Table 1).

Table 1. Look-up table of Manning's surface roughness coefficients (Source: Brunner, 2010b)

Land-cover Class	Equivalent or nearest Manning's *n* Class	Manning's roughness, *n*
Bare Soil	Bare soil	0.030
Built-up Areas	Concrete	0.019
Excavations	Dragline-excavated or dredged channel - No vegetation	0.028
Vegetation - Grasslands	Pasture no brush	0.038
Vegetation – High Density Shrubs and Trees	Heavy Stand of Timber	0.100
Vegetation – Light Density Shrubs and Trees	Light brush and trees	0.058
Vegetation - Medium Density Shrubs and Trees	Medium to Dense Brush and Trees	0.103
Vegetation - Aquatic	Dense weeds or aquatic plants in deep channels	0.035
Water Bodies	Natural channel, clean, winding, some pools and shoals	0.040

3.1.3 HEC RAS Model Configuration

The surface roughness map was used to assign Manning's *n* values to the cross-sections of the HEC RAS model. After this, the HEC RAS model was configured in a Hewlett Packard (HP) Z800 workstation. The configuration consisted of setting the HEC RAS model to accept water level data from the EFCOS WL monitoring stations MONTALBAN, STO NINO, and ROSARIO in near-real time. The WL data will serve as the model's boundary conditions.

By using WL data from the EFCOS Stations, HEC RAS will compute using its unsteady flow module the water profiles throughout the model domain in such a way that water level at the boundary condition points (i.e., the EFCOS stations) corresponds to the actual WL as recorded.

The WL recorded by the EFCOS stations at 10-minute interval are forwarded (via short-message-service, SMS) and stored in a data server in text format. The HEC RAS model, however, requires that the input files be in the HEC-Data Storage System (DSS) format. HEC-DSS is a data base system that was specifically designed to store data for applications in water resources (Brunner, 2010a). It can store almost any type of data, but it is most efficient at storing large blocks of data (e.g., time-series data). The conversion of the text files of WL records to HEC-DSS was implemented using a Jython script. The script, which was written by the Grid Operations Team of DOST-ASTI, works by first downloading the text files, reformatting them to comma-space-value (csv), and then converting to the HEC-DSS format. The script runs every 10 minutes so that new WL records at each station are added to the HEC-DSS file. If the station failed to send to the server new WL records, the entry in the HEC-DSS file will be left empty. However, these entries are filled later once the records have been successfully sent to the

server. In cases when the WL sensors failed to record WL data, the DSS conversion script will automatically fill-in the missing values using linear interpolation technique. The DSS files are stored in a separate server.

3.2 Flood model automation to generate and publish flood extent map

Figure 5 depicts the series of steps to generate and publish flood extent maps of Marikina River in near-real time at 10-minute intervals.

The series of steps can grouped into 3: (i.) download of DSS files to update the WL data at the boundary condition points, (ii.) update the model's initial condition using the output of the previous model run, running the model for the current time, and producing a flood extent shapefile within HEC RAS, (iii.) converting and publishing the flood extent shapefile as KML/KMZ in the Project NOAH website. Project NOAH stands for Nationwide Operational Assessment of Hazards. The generated flood extent map can be viewed by opening http://noah.dost.gov.ph/ and selecting Flood Maps → Flood Inundation Monitoring → Marikina River.

The series of steps were automated using the *GNU wget (*www.gnu.org/software/wget/*)* to download the DSS files; *AutoIt* (www.autoitscript.com) to run the HEC RAS model and generate flood extent shapefile; and *python* (www.python.org) to convert the shapefile to KML/KMZ and upload to the Project NOAH website). All the scripts were implemented in sequence and repeats every 10 minutes using Windows Task Scheduler.

The generation of flood extent shapefile is done using RASMapper, a post-processing module of HEC RAS. Here, the updated LiDAR DEM is used for flood inundation analysis which involves overlaying the water profile simulated by the model and computing for the flood depth. The shapefile of the extent of the flooded areas is automatically created.

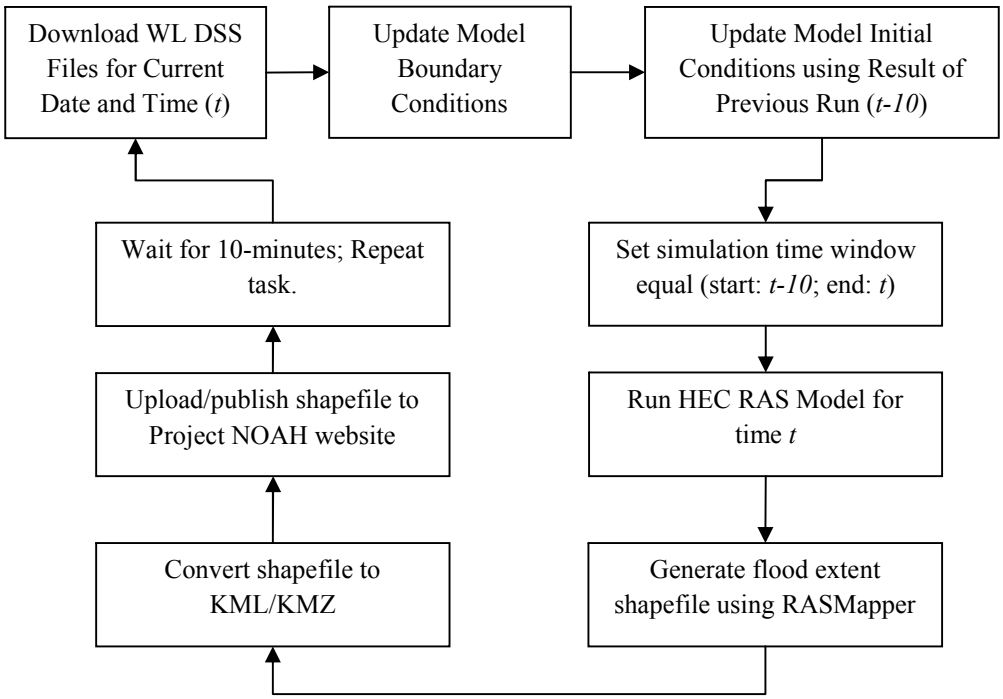

Figure 5. The series of steps implemented in the Marikina River Flood Extent Monitoring System to generate and publish flood extent maps in near-real time and for every 10 minutes.

3.3 Model testing and accuracy assessment

Before its deployment as a flood extent monitoring system, manual runs of the HEC RAS model were done to check model stability, and to check the accuracy of the simulations. The June 15-21, 2012 event was used in the accuracy assessment. During this period, water level sensors were deployed at the Tumana Station which is located approximately 9.5 km upstream of the Rosario Station. Model performance statistics such as Nash-Sutcliffe

Coefficient of Model Efficiency (*E*), average error, and root-mean-square error (RMSE) were computed to assess the accuracy of water levels simulated by the model.

4. RESULTS AND DISCUSSIONS

4.1 Land-cover map from the ALOS AVNIR-2 image

Figure 6 shows the land-cover map derived from the analysis of the processed ALOS AVNIR-2 satellite image. The map has an overall accuracy of 92.3% based on 1,000 random samples. This measure of accuracy does not include those classes that were manually digitized such aquatic vegetation, water bodies, exposed river beds and excavations. These particular land-cover classes are assumed to be 100% correct as they were thoroughly digitized from the images.

The classification error matrix is shown in Table 2. For the land-cover classes mapped using Maximum Likelihood classification, the Producer's and User's Accuracies for each land-cover class is more than 85%. The bare soil class has the lowest Producer's Accuracy (PA) of only 85.20%. The PA for built-up areas, grassland and the combined dense vegetation classes (high density, medium density and low density shrubs and trees) were more than 90%. The User's Accuracy (UA) for built-up areas is the lowest at 87.45%. Based on the producer's and user's accuracy, the land-cover map has an acceptable level of accuracy.

The land-cover map shows that built-up areas dominate most of the model domain, followed by grassland, bare soil, and low density shrubs and trees.

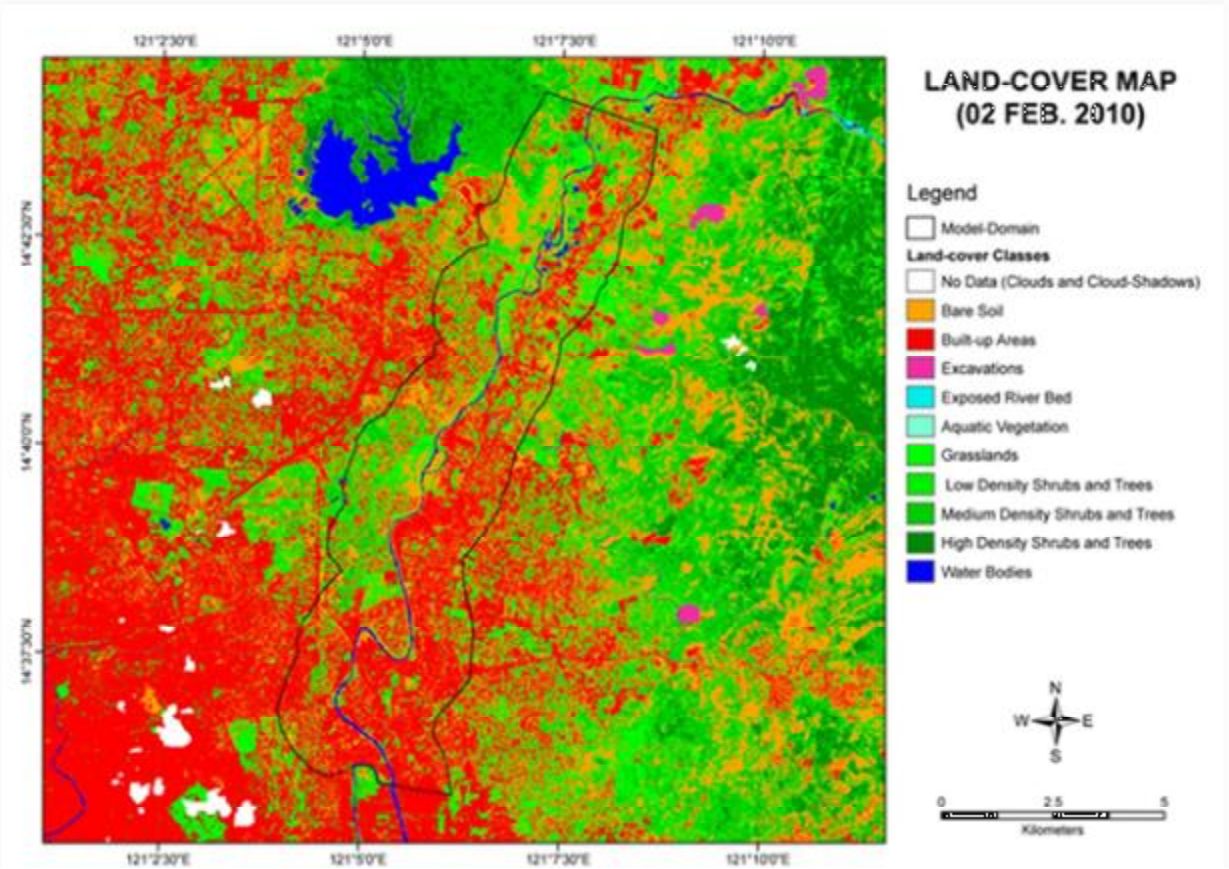

Figure 6. The land-cover map derived from the analysis of the processed ALOS AVNIR-2 satellite image.

Table 2. Error matrix of the ALOS AVNIR-2 land-cover classification.

	Land-cover Class	Ground Truth Pixels				
		Built-up Areas	Bare Soil	Grassland	Dense Vegetation	Total
Classified Pixels	Built-up Areas	237	32	2	0	271
	Bare Soil	12	213	6	0	231
	Grassland	1	4	227	4	236
	Dense Vegetation*	0	1	14	246	262
	Total	250	250	250	250	1000
	Producer's Accuracy	94.80%	85.20%	90.80%	98.40%	
	User's Accuracy	87.45%	92.21%	96.19%	93.89%	

*Dense vegetation = combined high density, medium density and low density shrubs and trees.

4.2 Surface roughness map for HEC RAS model parameterization

Figure 7 shows the surface roughness map generated by assigning Manning's roughness coefficient values to the land-cover classes. This map shows that the model domain has low roughness coefficients which indicate that the surface is relatively smooth compared to areas outside of it, especially on the eastern side. The domination of built-up areas within the model domain is the reason for the low roughness coefficients. Surfaces with low roughness coefficients mean that water can flow faster because the resistance by the surface is slow. This implies that during flooding, water can flow faster in the model domain and can affect more areas in little time.

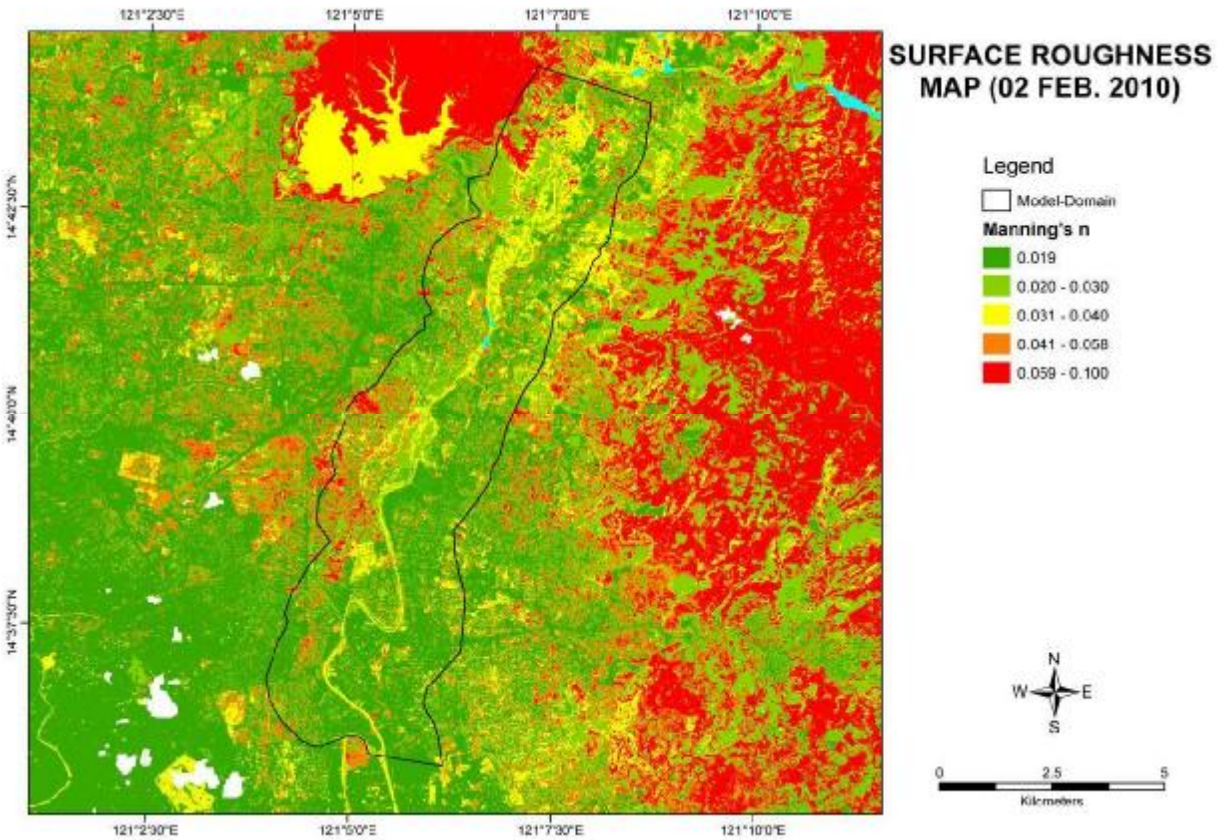

Figure 7. The land-cover map derived from the analysis of the processed ALOS AVNIR-2 satellite image.

4.3 The Marikina River Flood Extent Monitoring System

Figure 8 shows the hardware setup and interface of the flood extent monitoring system. The hardware is presently located at the Research Laboratory for Applied Geodesy and Space Technology, Training Center for Applied Geodesy and Photogrammetry & Department of Geodetic Engineering, University of the Philippines, Diliman.

The system has been active since June 2012 and has continuously provided near real time flood extent maps up to the present through Project NOAH. In fact, the system became valuable during the Southwest Monsoon Event last August 2012 when heavy rains comparable in volume to TS Ketsana caused flooding in Marikina River and other areas in Metro Manila. The system provided the public flood extent maps every 10 minutes and showed how flooding expanded from the banks of the Marikina River towards many populated areas. It also showed how flooding has receded after the event.

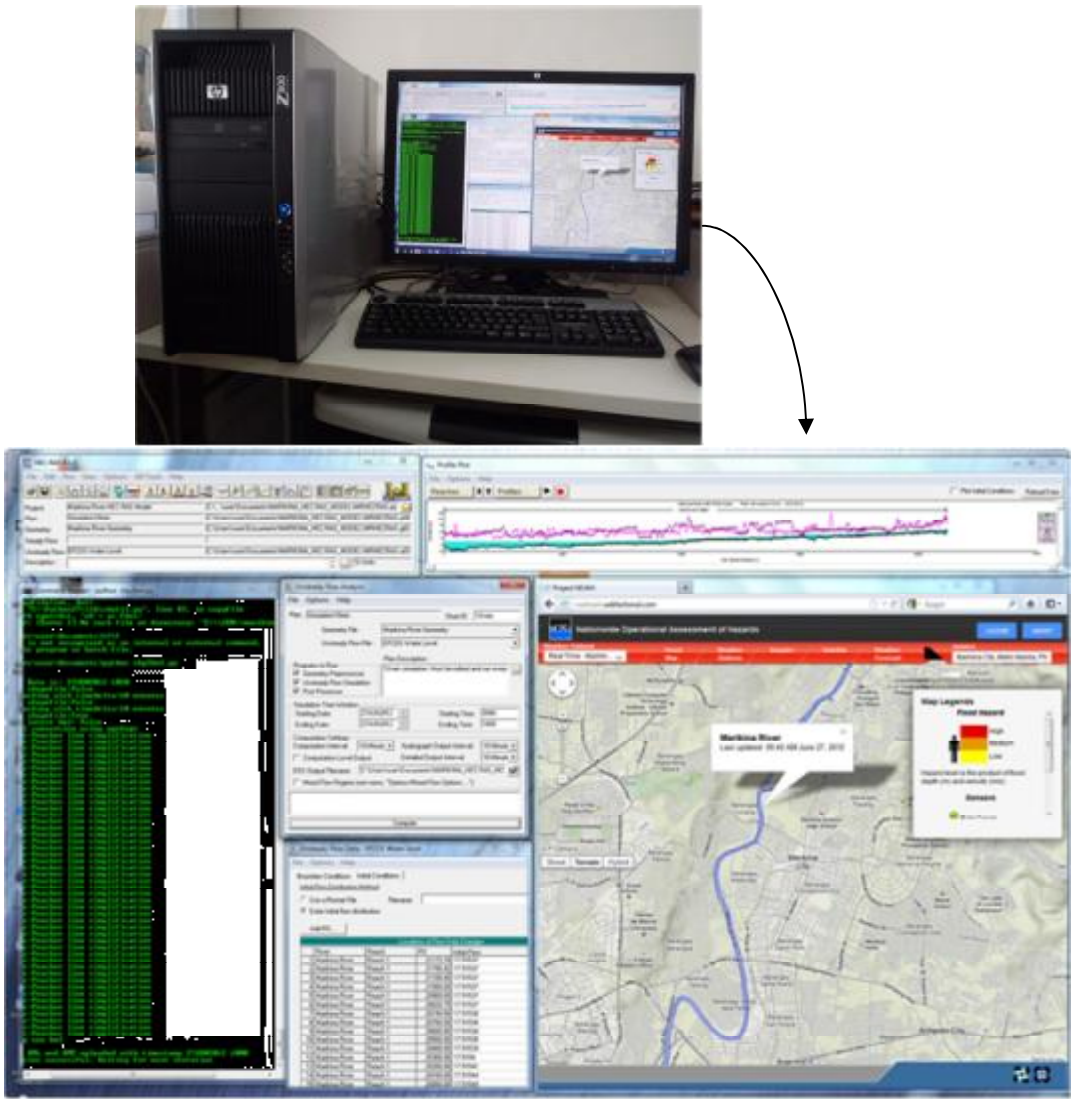

Figure 8. Top: The hardware setup of the Marikina River Flood Extent Monitoring System. Bottom: A screen shot of the interface of the system. The near-real time flood extent map (updated every 10 minutes) is available at the Project NOAH website, http://noah.dost.gov.ph.

4.4 Accuracy of the Simulated Water Levels

The comparison between the measured water level at Tumana Station and the simulated water level by the HEC RAS model is shown in Figure 9. It appears that the model has satisfactory performance, with Nash-Sutcliffe Model Efficiency of 0.88. Despite of this, improvement of the model through calibration and further validation is necessary because the model seems to overestimate water levels before and after the peak. The average error of -0.16 m indicates that the simulated water level is approx. 16 cm higher than the actual level (error = actual – simulated WL).

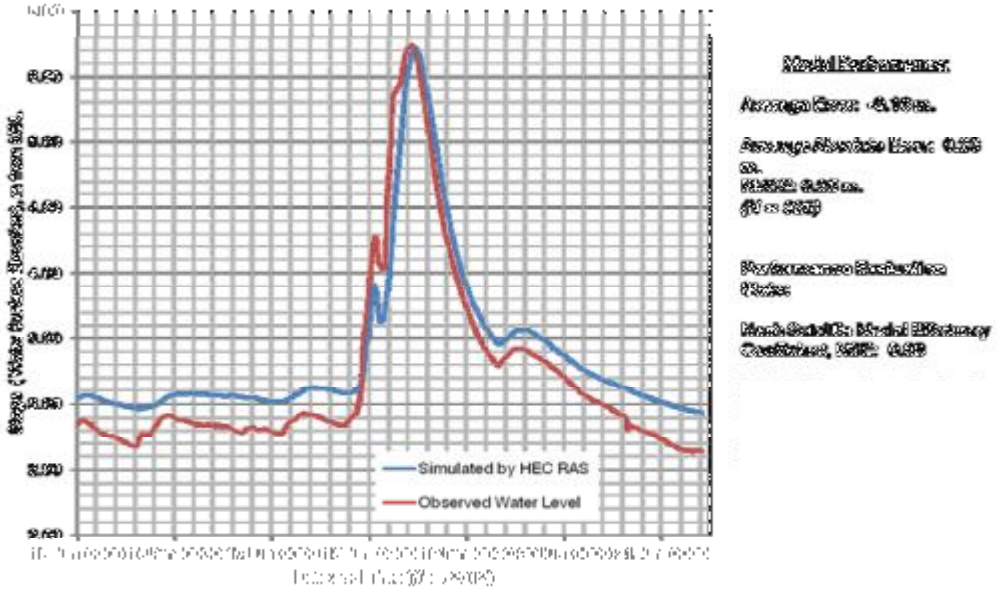

Figure 9. Graph showing the comparison between actual water levels (in red) and water levels simulated by the HEC RAS model at Tumana Station.

5. CONCLUSIONS

In this paper, we have presented the development of the Marikina River Flood Extent Monitoring System which aims to provide near-real time information on the status of flooding all throughout the river. The system made use of remote sensing and GIS technologies, especially in model preparation and parameterizations, as well as in providing near-real time outputs for viewing by the public. The system is useful especially if one wanted to know the current extent of flooding along the river and the areas that are presently flooded. Presently, the HEC RAS flood model is being calibrated and is to be coupled with a hydrologic model based on HEC HMS in order to forecast flood extent and depths based on forecasted rainfall depth and duration.

ACKNOWLEDGEMENT

We thank the Philippine's National Mapping and Resource Information Authority for providing the ALOS AVNIR2 satellite image, and the Collective Strengthening of Community Awareness for Natural Disasters (CSCAND) agencies for allowing us to use the LiDAR digital elevation dataset. This paper is one of the outputs of an on-going project entitled "Modeling of Flashflood Events using Integrated GIS and Hydrological Simulations" under the "Surveys and Measurement Technologies for Flood Control, Mitigation and Management System" program being funded by the Philippine Council for Industry, Energy and Emerging Technology Research and Development of the Department of Science and Technology (PCIEERD-DOST).

REFERENCES

Abon, C.C., David, C.P.C., Pellejera, N.E.B., 2011. Reconstructing the Tropical Storm Ketsana flood event in Marikina River, Philippines. Hydrology & Earth System Sciences, 15, pp. 1283–1289.

Badilla, R.A., 2008. Flood modeling in the Pasig-Marikina River Basin. MSc Thesis, International Institute for Geo-Information Science Earth and Observation , Enschede, The Netherlands.

Bouvet, M., Goryl, P., Chander, G., Santer, R., Sauiner, S., 2007. Preliminary radiometric calibration assessment of ALOS AVNIR-2. In: Proceedings of the IEEE International Geoscience and Remote Sensing Symposium – IGARSS 2007, pp. 2673-2676.

Brunner, G.W., 2010a. HEC RAS River Analysis System User Manual, version 4.1 January 2010, US Corps of Engineers, Institute of Water Resources, Hydrologic Engineering Center, Davis, California.

Brunner, G.W., 2010b. HEC RAS River Analysis System Hydraulic Reference Manual. US Corps of Engineers, Institute of Water Resources, Hydrologic Engineering Center, Davis, California.

Cheng, M.H., 2009. Natural disasters highlight gaps in preparedness. The Lancet, 274, pp. 1317-1318.

Elumnoh, A., Shrestha, R.P., 2000. Application of DEM data to Landsat image classification: evaluation in a tropical wet-dry landscape of Thailand. Photogrammetric Engineering & Remote Sensing, 66(3), pp. 297-304.

Fitzpatrick-Lins, K., 1981. Comparison of sampling procedures and data analysis of a land-use and land-cover map. Photogrammetric Engineering & Remote Sensing, 47, pp. 349-366.